

Modeling and Controlling the Spread of Epidemic with Various Social and Economic Scenarios

S. P. Lukyanets,¹ I. S. Gandzha,¹ and O. V. Kliushnychenko¹

¹*Institute of Physics, Nat. Acad. of Sci. of Ukraine, Prosp. Nauky 46, Kyiv 03028, Ukraine*^{*}

(Dated: June 16, 2020)

We propose a novel model for describing the spreading processes, in particular, epidemics. Our model is an extension of the SIQR (susceptible-infected-quarantine-recovered) and SIRP (susceptible-infected-recovered-pathogen) models used earlier to describe various scenarios of epidemic spread. As compared to the basic SIR model, our model takes into account two possible routes of virus transmission: direct from the infected compartment to the susceptible compartment and indirect via some intermediate medium or fomites. The transmission rates are estimated in terms of the average distances between the individuals in selected social environments and characteristic relaxation times. We also introduce a resource activation function that reflects the load of the epidemics on economics and the limited capacity of the medical infrastructure. Our model brings an advantage of building various control strategies to minimize the effect of the epidemic and can be applied to modeling the recent COVID-19 outbreak.

I. INTRODUCTION

As widely acknowledged [1–5], the spread of information, rumors, ideas, or deceases share many similarities and, in most cases, spreading processes are governed by similar models.

There are entire classes of models in terms of complexity or approximations to describe the spreading processes, starting from dynamic systems, e.g. [6–13], that stem from classical works [14–18]. More complex models include stochastic effects, e.g. [19]; models with spatial flows, e.g. diffusion [20]; and models allowing for non-trivial spatial structure or topology, e.g. [1, 21]. One common feature in the majority of these models is the presence of kinetic coefficients or parameters that characterize the probability of elementary processes or reactions per unit time. On the one hand, these model parameters (constants) determine the instability points and characteristic rates of instability growth. On the other hand, however, the kinetic coefficients or probabilities are not the proper control parameters that are readily available, and they can only be estimated indirectly in terms of other parameters.

The dynamics of any spreading process, e.g. an epidemic, is determined by the individual peculiarities of people in the selected social group, by the type and mechanism of infection, etc. To describe such a process, it is necessary to indicate some ways for a specific influence on the process by selecting, in particular, a proper quarantine strategy. A dramatic example is the spread of COVID-19, when different countries resort to different quarantine measures [22]. Such measures are controlled by the choice of certain parameters available to society (e.g. working day duration, average density of people in public places, frequency of disinfection, intensity of

transport communications, etc.). The problem of strategy selection reduces to problems of optimal control theory for feedback systems (theory of games in the more general case [23]). An important point in strategy selection is to single out the control parameters that are readily available in the system.

One of the basic constants in spreading models is the reaction cross-section or its characteristic rate. For instance, the infection reaction is associated with scattering of the infected individuals on the spatiotemporal fluctuations of population density. As is well-known [24], the infection probability depends on population density non-monotonically. At low densities, the low probability of scattering of the infected individuals on the susceptible individuals results in a small total cross-section of the infection reaction. At high densities, the mobility of spreaders decreases, and it mitigates the spreading process. Moreover, the scattering of spreaders on local population-density fluctuations should determine the critical concentration of secondary infected cases sufficient for the initiation of the collective process, i.e. epidemic. In general, kinetic description of spreading is quite a complex problem that needs to account for the changes of the internal state of the spreaders in the course of collisions as well as the presence of spatial inhomogeneity in the system and its non-equilibrium properties.

The similar remarks can be made in regard to the characteristic relaxation times, e.g. the characteristic rehabilitation or recovery rates. These parameters are determined by the individual peculiarities of the person and generally are not social group dependant. In addition, it is determined by the quality of the provision of medical services and food. The quickest recovery depends on the cost of medical services, the bare subsistence level of consumption, E , and the availability of some resource ρ , e.g. money [25]. Since the cost of services is fixed, the service is terminated if there is not enough personal, private, or collective financial resource ($\rho \ll E$). In other words, there is an analog of some energy barrier, with the

^{*} lukyan@iop.kiev.ua gandzha@iop.kiev.ua kliushnychenko@iop.kiev.ua

parameter E serving as its height. Therefore, it can be assumed that the rehabilitation rate should have an activation character, $\sim \exp(-E/\rho)$, similar to the temperature dependence of the activation process with activation energy E , see, e.g., [26–28].

The presence of activation process indicates that the system can be subjected to the so-called explosive instability. For example, when a chemical reaction occurs with the release of heat and has an activation character, it goes faster at higher temperatures. This leads to yet greater temperature increase and, as a result, to the so-called Zeldovich–Frank–Kamenetskii explosive instability [29–31]. The fight against the epidemic involves additional costs, e.g. associated with quarantine measures, which result in the reduction of the production of the collective formal resource ρ . The resource being depleted, the quality of medical services and the rehabilitation (recovery) rate drop. As a result, the number of active members in the population goes down. This, in turn, leads to a further decline in the collective resource production, with the level of income needed for basic survival being lower and lower. Such a scenario finally results in the total collapse of the system.

In this paper, we try to address the points mentioned above. In other words, we are interested not only in modeling the spreading process but also in identifying the ways it can be controlled by socially available parameters and which consequences such control measures can lead to. To demonstrate a number of possible effects, we turn to the simplest feedback model that is based on dynamical systems. We would like to mention two features of this model.

(I) In order to take into account the fact that an individual can stay in different environments or public places (e.g. transport, shops, work) that are characterized by different densities of surrounding individuals, it is convenient to consider the selected social group and its average daily cycle (T). For instance, we can introduce the average daily time slots the individual spends at home (T_1), at shop or other public places (T_2), in transport (T_3), at work (T_4), etc. and define (at least under normal conditions) the characteristic density c_j of individuals or the average distance $\overline{\ell_j}$ between them. We also make a qualitative assessment of the dependence of the reaction (infection) rate on the density of individuals or average distance between them in order to clearly identify the set of control parameters $\{T_j, \ell_j\}$. Finally, we take into consideration a possibility of indirect transmission through the medium (e.g. contaminated water [32, 33]) or via the so-called fomites [34, 35]. The indirect transmission rate is determined by $c_j(\overline{\ell_j})$ as well.

(II) The relationship between economics and epidemic is taken into account by means of the above-mentioned activation mechanism $\sim \exp(-E/\rho)$ for the characteristic relaxation times. To this end, we use the simplest form of the equation for the dynamics of the formal resource ρ .

Before we proceed to the consideration of our main

model described in Sect. IV, we make an attempt to understand the effect of the relaxation activation mechanism when the system can pass through a number of quasi-stable states and then collapse. In this case, its dynamics resembles the so-called devil's staircase [36] providing a clear illustration to the global pandemic scenario of the world never being the same again after the epidemic. To this end, we turn to a simple toy model that accounts for a formal demographic and economic resource and is more suitable for describing a primitive community or family.

II. A SIMPLIFIED MODEL WITH ACTIVATION MECHANISM

We first consider a simplified model where some social group of individuals is subdivided into two compartments: susceptible (S) and infected (I). The susceptible individuals are infected at some transmission rate β , which is defined as a product of the contact rate and the probability that a contact of infected individual with a susceptible individual results in transmission. The infected individuals recover and become susceptible again with some recovery rate Γ_i , which identifies the probability of recovery per unit time and is estimated as the reciprocal of the mean time spent in the infectious class. The recovery process is governed by the general economic situation described by some integral activation parameter E which reflects the cost of medical and other essential life services as well as the bare subsistence level of consumption. The corresponding mathematical model is given by the following two ODEs:

$$\begin{aligned} \partial_t s &= -\beta s (1 - s) + \Gamma_i e^{-E/\rho} (1 - s), \\ \partial_t \rho &= G s - \Gamma_\rho \rho - \Lambda, \end{aligned} \quad (1)$$

where the operator ∂_t stands for the derivative with respect to time t . Here s is the number density of susceptible individuals and $i = 1 - s$ is the number density of infected individuals. The total number of susceptible and infected individuals is assumed to be constant. The initial conditions at $t = 0$ are taken as

$$s(0) = 1 - i_0, \quad i(0) = i_0, \quad \rho(0) = \rho_0, \quad (2)$$

i_0 being the initial number density of infected individuals.

The function ρ represents some general “resource”. Formally it corresponds to the collective product or earned money. The production of this resource per unit time is proportional to the number density of working individuals, s (the infected individuals are assumed to be not working). The constant G formalizes the resource volume generated by them per unit time. The second term, $\Gamma_\rho \rho$, formally describes the collective expenses or taxes. Roughly speaking, the expenses are assumed to be proportional to earnings. Thus, the coefficient Γ_ρ represents the resource consumption rate. The last term Λ represents the fixed expenses necessary for keeping some infrastructure (e.g. amortization, municipal services, etc.).

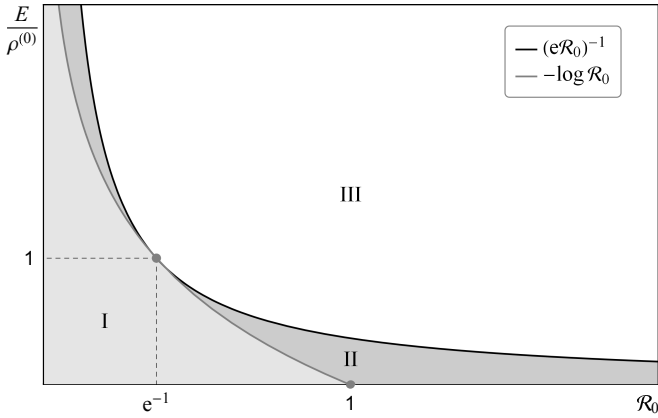


Figure 1. Phase diagram with three possible states (for the case $\Lambda = 0$): disease-free equilibrium (I), endemic equilibrium (II), and collapse (III).

In the case of unlimited resource ($E \ll \rho$), the equation for s reduces to the basic SIS (susceptible-infected-susceptible) model, whose solutions are well studied [10, 11, 17]. The purpose of this paper is to investigate the effect of nonzero activation parameter E (which we will also refer to as “activation energy”) on the dynamics of epidemic described by system (1).

As we understand, if there are no black swan events like the epidemic, there exists a quasi-stationary equilibrium state with $\rho = \rho^{(0)} = \text{const}$. It is called the disease-free equilibrium and is given by the trivial stationary solution of Eqs. (1):

$$s^{(0)} = 1, \quad \rho^{(0)} = \frac{G - \Lambda}{\Gamma_\rho}. \quad (3)$$

On the other hand, under the stress situations like epidemic, the system can go out from the disease-free equilibrium, with resource depleted. Indeed, another stationary solution to the equation for ρ is given by

$$\rho^* = \frac{G s^* - \Lambda}{\Gamma_\rho}, \quad (4)$$

where s^* is given by the following transcendental equation:

$$\frac{G s^* - \Lambda}{\Gamma_\rho} \log(\mathcal{R}_0 s^*) = -E. \quad (5)$$

The parameter

$$\mathcal{R}_0 = \frac{\beta}{\Gamma_i} \quad (6)$$

is the basic reproduction number. It defines the average number of transmissions one infected individual makes in the entire susceptible compartment during the entire time of being infected. When $\mathcal{R}_0 \leq 1$, the disease-free equilibrium is stable, and there is no epidemic outbreak. When $\mathcal{R}_0 > 1$, the disease-free equilibrium is unstable, and

the system evolves to the new equilibrium state $\{s^*, \rho^*\}$ called the endemic equilibrium [10, 11].

When $E = 0$, Eq. (5) has two solutions. The first solution,

$$s^* = \mathcal{R}_0^{-1}, \quad (7)$$

is stable at $\mathcal{R}_0 > 1$ and defines the endemic equilibrium point. The second solution $s^* = \frac{\Lambda}{G}$ is unstable for all \mathcal{R}_0 .

To simplify our further analysis for the case $E > 0$, we put $\Lambda = 0$. Then Eq. (5) can be rewritten in a simpler form:

$$z \log z = -\mathcal{E}, \quad (8)$$

where

$$z = \mathcal{R}_0 s, \quad \mathcal{E} = E \frac{\mathcal{R}_0}{\rho^{(0)}}. \quad (9)$$

For $0 < \mathcal{E} < \mathcal{E}_c$, where $\mathcal{E}_c = e^{-1} \approx 0.368$, Eq. (8) has two solutions: $z_1 > \mathcal{E}_c$ (which defines the endemic equilibrium point) and $0 < z_2 < \mathcal{E}_c$ (which is always unstable). For $\mathcal{E} = \mathcal{E}_c$, there is one solution $z_{1,2} = \mathcal{E}_c$. Finally, there are no real solutions for $\mathcal{E} > \mathcal{E}_c$.

The last case is most important for our consideration. It means that at some E and \mathcal{R}_0 there is no stable endemic equilibrium because of resource depletion, and the dynamical system described by Eqs. (1) should collapse (such a situation is sometimes called the explosive instability). The critical activation energy at which the system starts to collapse is given by a formula

$$E_c = \rho^{(0)} (e\mathcal{R}_0)^{-1}. \quad (10)$$

Except for the condition $0 \leq E < E_c$, the endemic equilibrium point should also meet the requirement of $s^* < 1$, which effectively implies that $E < E_e$, where

$$E_e = -\rho^{(0)} \log \mathcal{R}_0. \quad (11)$$

Relations (10) and (11) define two critical curves in the (\mathcal{R}_0, E) plane which determine the evolution scenario for dynamical system (1). Depending on the values of parameters \mathcal{R}_0 and E , the system can evolve into three possible states: disease-free equilibrium, endemic equilibrium, or collapse. Figure 1 shows the corresponding phase diagram.

The above analysis is supported by the results of numerical integration of Eqs. (1) demonstrated in Fig. 2 (the case $\mathcal{R}_0 < 1$) and Fig. 3 (the case $\mathcal{R}_0 > 1$). In these examples we normalized the resource function by its trivial stationary value $\rho^{(0)}$, which is equivalent to taking $\rho^{(0)} = 1$. In this case we have $\rho^* = s^*$.

When $E = 0$, the dynamics of system (1) follows the basic SIS model. It evolves to the state of disease-free equilibrium at $\mathcal{R}_0 \leq 1$ [Fig. 2(a)] and to the state of endemic equilibrium at $\mathcal{R}_0 > 1$ [Fig. 3(a)].

When $E > 0$, some part of the resource is consumed, and the number of healthy (susceptible) individuals decreases [Fig. 3(b)]. There is a critical value E_e defined by

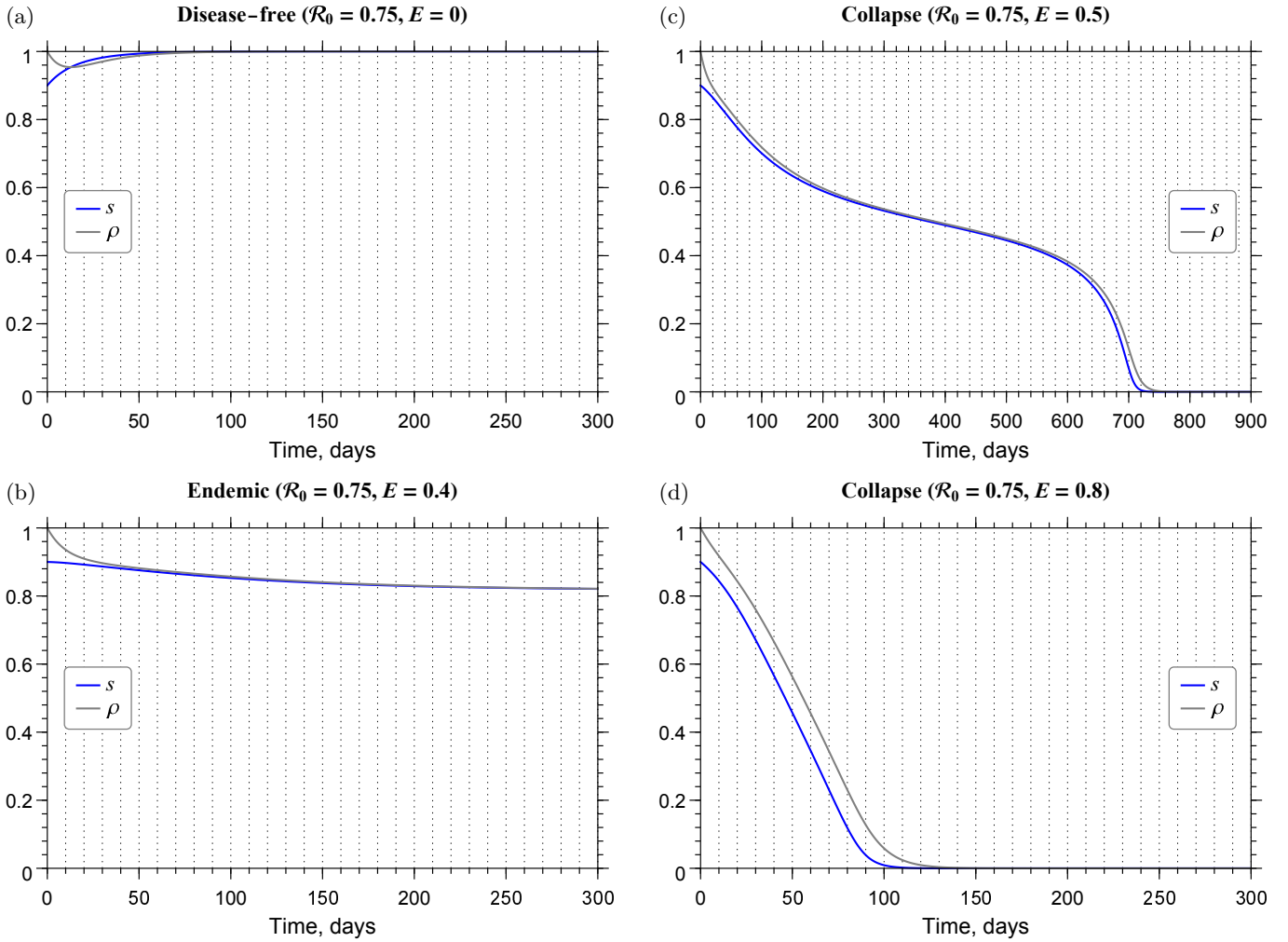


Figure 2. The number density of susceptible individuals and normalized resource function as functions of time in the case $\mathcal{R}_0 < 1$ ($\beta = 0.15 T^{-1}$). Other parameters were taken equal to $T = 1$ day, $\Gamma_i = 0.2 T^{-1}$, $\Gamma_\rho = G = 0.1 T^{-1}$, $\Lambda = 0$. The initial conditions are $i_0 = 0.1$, $\rho_0 = 1$.

formula (11) at which the system evolves to the endemic equilibrium even at $\mathcal{R}_0 < 1$ [Fig. 2(b)]. This scenario is impossible in the basic SIS model. When the activation energy is further increased and becomes larger than the critical value E_c defined by formula (10), the endemic equilibrium is no longer stable and the system collapses to the state $s^* = \rho^* = 0$ [Fig. 2(c,d)]. This means that all the individuals become infected and there is no resource to reverse the epidemic back. The same scenario is observed in the case $\mathcal{R}_0 > 1$ [Fig. 3(c,d)].

When E is above the critical value E_c but still close to it, the system first tries to occupy the quasi-stationary endemic state (which is unstable). This process can take quite a long time and then the system finally collapses [Figs. 2(c) and 3(c)]. It resembles the well-known “devil’s staircase” pattern [36]. At larger activation energies, the collapse is very fast with no intermediate quasi-stationary evolution [Figs. 2(d) and 3(d)].

The simplified SIS-like model and example considered

in this Section demonstrate that in the case of limited resource ($E > 0$), there exists a certain critical point for any basic reproduction number \mathcal{R}_0 at which the system collapses and can no longer stabilize and return to the stable pre-epidemic or after-epidemic state. This fact provides a clear illustration to the global pandemic scenario of the world never being the same again after the epidemic.

III. SOCIAL CONTROL PARAMETERS

As mentioned above, the spreading process can be controlled only by accessible for society parameters. These parameters are, e.g. the mean distance between individuals and the mean time spent in a particular place.

In order to take into account the fact that an individual can stay in different environments or public places (e.g. transport, shops, work) that are characterized by

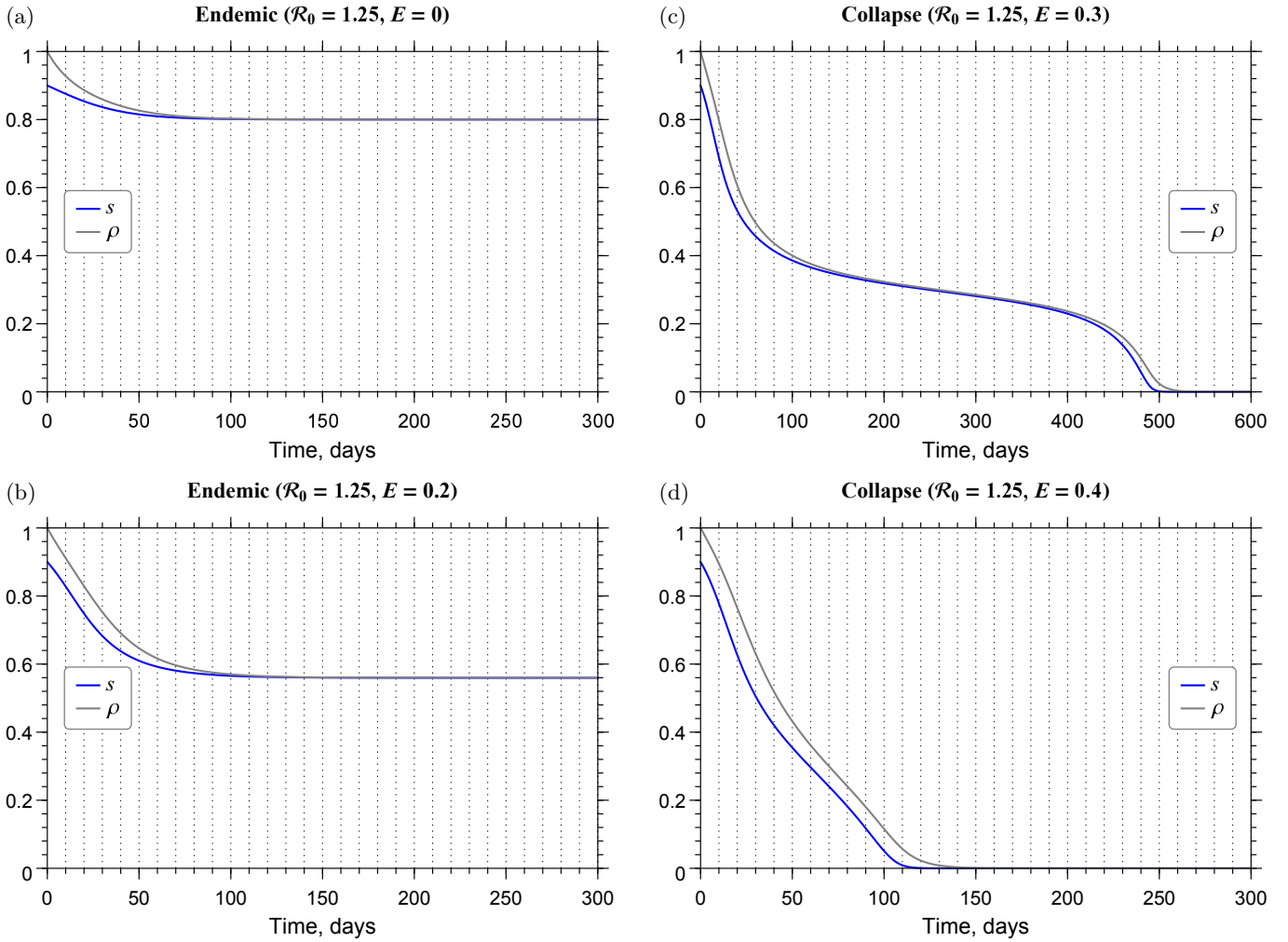


Figure 3. The number density of susceptible individuals and normalized resource function as functions of time in the case $\mathcal{R}_0 > 1$ ($\beta = 0.25 T^{-1}$). Other parameters are the same as in Fig. 3.

different densities of surrounding individuals, it is convenient to consider the selected social group and its average daily cycle (T). For instance, we can introduce the average daily time slots the individual spends at home (T_1), at shop or other public places (T_2), in transport (T_3), at work (T_4), etc. and define (at least under normal conditions) the characteristic density c_j of individuals or the average distance $\bar{\ell}_j$ between them. We also make a qualitative assessment of the dependence of the reaction (infection) rate on the density of individuals or average distance between them in order to clearly identify the set of control parameters $\{T_j, \bar{\ell}_j\}$. We estimate the reaction cross-section, using a simple approach, in order to take into account a safe distance, and consider also the additional mechanical infection associated with infecting by the environment. The latter is also depends on the population density in a given place. Such approach allows not only to single out the characteristic parameters one can influence, but also to describe, in the same respect, another social groups, e.g. the category of people that

go to work in the subway, with high population density, or by car, taking into account their intersecting points. When determining the chemical reaction cross-section via a field or some mediator, we deal with parameters which should be obtained from general considerations. For example, the probability to be infected per unit time for an individual in the vicinity of infected one for a certain period of time which depends on the individual organism resistance.

Here, we roughly estimate the dependence of mean infection rate ω_j (reaction rate) on characteristic distance between people for an individual in a “social” region (location) “ j ” with a given mean population density $\bar{c}_j \sim (\bar{\ell}_j)^{-2}$, where $\bar{\ell}_j$ is the mean distance between them.

In general case, the probability of being infected (“interaction potential”) depends on the distance between infected and susceptible, and, as may be assumed, is a damped function with a characteristic correlation radius (decay length) ℓ_c . Then, the scattering (reaction) cross-section is determined by the probability of finding the

infected individual at a certain distance from susceptible one and by the interaction potential. By averaging over all the configurations of spatial locations of infected, susceptible and immune individuals, we obtain the characteristic infection rate ω_j which depends on $\bar{\ell}_j$ and ℓ_c . In the case of non-trivial spatial structure (topology) of population, the scattering problem is correctly described by the two-point correlation function or so-called structure factor.

However, for simplicity, here we assume that the elementary infection act probability for susceptible individual, falling into the vicinity of radius ℓ_c around the infected one, does not depend on the distance and equals ω . We also assume that the event of being infected from two different infected individuals are independent. In what follows, ℓ_c is associated with socially safe distance.

For simplicity, we suppose that, for each social zone j , the mean population density is fixed under any social conditions. The mean number of persons falling into the area of radius ℓ_c around susceptible individual is $\bar{N}_j \approx \bar{c}_j \pi \ell_c^2$. One can estimate the infection probability of susceptible individual per unit time $\Delta P_j = \omega q(\bar{N}_j - 1)$, where $q \approx I/N$ is the probability to be infected. By summing over all the susceptible individuals in the system, we obtain the characteristic growth rate of the number of infected individuals, $S \Delta P_j$, in the system with population density c_j . By dividing on the total population number N , the rate of infection reaction in the region with density c_j takes the form

$$\frac{i}{\Delta t} \approx \omega(\bar{N}_j - 1)si, \quad (12)$$

i.e.

$$\omega_j = \omega(\bar{N}_j - 1) \approx \omega \left(\left(\frac{\ell_c}{\bar{\ell}_j} \right)^2 - 1 \right) \quad (13)$$

Here s is the number density of susceptible individuals and i is the number density of infected individuals. We can estimate the relative error for ω_j caused by fluctuation of the number of individuals falling into the area of radius ℓ_c by using, for simplicity, a triangular lattice with a lattice constant ℓ_0 (characteristic size of the individual). The deviation of squared number of particles $\overline{\Delta N^2} = \overline{N^2} - \overline{N}^2$:

$$\overline{\Delta N^2} = \theta N_m + \theta^2 N_m(N_m - 1) \approx \theta N_m \approx \overline{N}$$

where θ is the probability that lattice site is occupied by a person, and N_m is the maximal number of persons that can fall into the area of radius ℓ_c :

$$N_m \approx 1 + 6 \left(\frac{\ell_c}{\ell_0} \right) \left(\frac{\ell_c}{\ell_0} + 1 \right)$$

Then, the relative error for ω_j can be estimated as $\delta \omega_j / \omega_j = \sqrt{\overline{\Delta N_j^2}} / \overline{N_j} \sim \left(\sqrt{\overline{\Delta N_j}} \right)^{-1} \sim \bar{\ell}_j / \ell_c \sim 10^{-1}$.

assuming that $\ell_c \sim 4m$, and minimal distance between persons $\ell_0 \sim 1m$, and $\ell_0 < \bar{\ell}_j < \ell_c$. Generally, it should be noted that characteristic reaction cross-section can have more complex dependence on density $\sim c^\alpha$, $1 \leq \alpha \leq 3$, and other type of non-linearity than si [57].

Next we roughly estimate the probability of elementary infection act ω . Let ℓ_0 be the minimum possible distance between two individuals. Assume that the suspected individual is infected with probability $p_0 = 1$ if he stays at the distance ℓ_0 from the infected individual for some characteristic time τ_{is} (e.g. 8 hours). Then the probability of becoming infected at the minimum distance per unit time is $\omega = a / \tau_{is}$. The parameter a can be estimated as the ratio of the “contact” area between the susceptible and infected individual to the total area determined by the correlation radius ℓ_c : $a \approx \ell_0 / \ell_c^2$.

Then we assume that each individual can stay in N_ω different locations during some typical period of time T (e.g. one day). Each location is characterized by its own average distance $\bar{\ell}_j$. Then the integral transmission rate β for all locations is given by a formula:

$$\beta = \sum_{j=1}^{N_\omega} \omega_j \frac{T_j}{T}, \quad (14)$$

where T_j are the characteristic times spent in each of the locations j , with

$$\sum_{j=1}^{N_\omega} T_j = T. \quad (15)$$

In practice, we will limit ourselves by four locations ($N_\omega = 4$). Location 1 refers to staying at home (limited social contact), location 2 refers to shopping and other social contacts during a day, location 3 refers to staying in public transport (where the transmission probability is the highest), location 4 refers to staying at work.

Our estimates of the transmission frequencies ω_j and rates β for various sets of social control parameters T_j and $\bar{\ell}_j$ are given in Table II (see Appendix A). We considered three possible scenarios: casual (no restrictions), soft quarantine (social distancing in place), and strict quarantine (restricted public transport, limited social contacts, partial cutting of economic activity). The soft quarantine measures reduce the integral transmission rate β by a factor of 3, and the strict quarantine measures reduce it by a factor of 7. Thus, our rough estimates given by formulas (12) and (14) allow the transmission rates to be controlled by the proper choice of parameters T_j and $\bar{\ell}_j$ in different social scenarios. Our β estimates in the case of casual scenario fall in the range derived from the statistical data for the COVID-19 epidemic in the Wuhan city [37, 38].

IV. EXTENDED MODEL

A. Mathematical formulation

Here we consider a more realistic model of epidemic evolution. In addition to the direct transmission of infection by direct contact of the susceptible individual with the infected individual, we also consider the indirect transmission of the pathogen (e.g. virus) either through the medium (e.g. contaminated water [32, 33]) or via intermediate objects (like hands, counters, doorknobs, etc.) often called fomites [34, 35]. Such an intermediate medium or fomites will further be referred to as “cloud”. We associate a separate cloud with each social location j described earlier in Section II.

We subdivide the selected social group into five compartments: susceptible (S), infected (I), quarantine (Q), recovered (R), and deceased (F). The susceptible individuals (S) are those who are at risk to be infected. The infected individuals (I) are those who have been infected and pass through the virus incubation period. Then they either recover (with or without the acquired immunity) or pass to the severe form of decease (like fever or organ dysfunction) when they need to stay isolated either at home or at hospital getting a medical help. Such individuals are referred to as the quarantine individuals (Q). The quarantine individuals either recover (with or without the acquired immunity) or die. The corresponding mathematical model is given by the following system of ODEs:

$$\begin{aligned} \partial_t s &= -s \sum_j (\omega_j i + \Omega_j d_j) \frac{T_j}{T} + \Gamma_{is} i + \Gamma_{qs} e^{-E/\rho} q, \\ \partial_t i &= s \sum_j (\omega_j i + \Omega_j d_j) \frac{T_j}{T} - \Gamma_i i, \\ \partial_t q &= \Gamma_{iq} i - \Gamma_q q, \\ \partial_t r &= \Gamma_{ir} i + \Gamma_{qr} e^{-E/\rho} q, \end{aligned} \quad (16a)$$

where the functions $s(t)$, $i(t)$, $q(t)$, and $r(t)$ describe the number densities of the susceptible, infected, quarantine, and recovered compartments, respectively. Here the index $j = 1, \dots, N_\omega$ runs through all the social locations, and N_ω is the total number of such locations taken into consideration (see Section II). The average frequencies ω_j of infection transmission in each of the locations j are defined by formula (12). The typical characteristic times T_j spent in each of the locations j are given in Table II, the total time spent in all the locations being constant each day and equal to the day duration T [see Eq. (15)].

The number density of fatal cases is described by the function $f(t)$ that is determined by the equation

$$\partial_t f = \left(\Gamma_q + (\Gamma_{qf} - \Gamma_q) e^{-E/\rho} \right) q. \quad (16b)$$

Each of the functions $d_j(t)$ describes the density of pathogen per individual in the cloud j and contributes to

the indirect transmission of the infection from the cloud to susceptible individuals. The pathogen dynamics in the cloud j is given by the following equation:

$$\partial_t d_j = \sigma_j i - \gamma_j d_j. \quad (16c)$$

The first term, $\sigma_j i$, describes the pathogen shedding by the infected individuals into the cloud, and the second term, $\gamma_j d_j$, describes the pathogen decay in the cloud due to natural inactivation, decontamination, or other routes.

The resource function ρ and the activation parameter E have the same meaning as in Section III. The corresponding resource balance equation is

$$\partial_t \rho = G(s + i + r) - \Gamma_\rho \rho - \Lambda. \quad (16d)$$

The above equations are supplemented with the following initial conditions

$$\begin{aligned} s(0) &= 1 - i_0, \quad i(0) = i_0, \\ q(0) &= r(0) = f(0) = d_j(0) = 0, \quad \rho(0) = \rho_0. \end{aligned} \quad (16e)$$

The total number density is assumed to be constant:

$$s(t) + i(t) + q(t) + r(t) + f(t) = 1. \quad (17)$$

Effectively, our model is a combination or extension of simpler models like SIR (susceptible-infected-recovered) [6, 7, 10, 11, 16], SIRD (susceptible-infected-recovered-deceased) [39], SIQR (susceptible-infected-quarantine-recovered) [40], SIWR/SIVR/SIRP (susceptible-infected-recovered-pathogen) [32, 41–43], and EITS (environmental infection transmission system) [34].

B. Assumptions

1. The system is closed (no migration outside the selected population group and no one is added to the population).
2. The natural demography is ignored.
3. The uniform mixing of people is assumed (no uneven spatial distribution). The distribution of the pathogen in each cloud is assumed to be uniform.
4. The latent period from exposure to the onset of infectiousness is ignored, i.e. all the exposed individuals are assumed to be infected and can infect others. The SEIR (susceptible-exposed-infected-recovered) model was demonstrated to have no practical advantage as compared to the SIR model [37].

C. Parameters

The full description and indicative values of the parameters of Eqs. (16) are given in Table III (Appendix A).

In particular, the parameter Γ_{is} describes a rate (we call it the relaxation frequency) at which the infected individuals recover without acquiring the immunity and come back to the susceptible compartment. The parameter Γ_{iq} describes a rate at which the infected individuals develop the severe condition and pass to the quarantine compartment, where they become isolated either at home or at hospital. The parameter Γ_{ir} describes a rate at which the infected individuals recover without complications and acquire the immunity. It is proportional to the probability μ of acquiring the immunity (see Table III). The relaxation frequency Γ_i is defined as follows:

$$\Gamma_i = \Gamma_{iq} + \Gamma_{ir} + \Gamma_{is} = \tau_i^{-1},$$

where τ_i is the characteristic pathogen incubation period.

The parameters Γ_{qr} and Γ_{qs} describe the rates at which the quarantine individuals recover with or without the acquired immunity. The parameter Γ_{qf} describes the fatality rate in the case of unlimited resource ($E \ll \rho$). This case models a situation when the quarantine individuals all get the necessary medical care and the fatalities are only attributed to insuperable health complications (such as concomitant diseases or age factor). In the opposite case, when $E \gg \rho$, the fatality rate is at its maximum and is equal to the total relaxation frequency for quarantine individuals,

$$\Gamma_q = \Gamma_{qr} + \Gamma_{qs} + \Gamma_{qf} = \tau_q^{-1},$$

where τ_q is the average quarantine/hospitalization period. This case refers to the collapse of the medical system when the quarantine individuals get no medical help or treatment.

Each of the parameters Ω_j describes the typical frequency of the pathogen transmission from the cloud j to the susceptible individual. Two other cloud-related parameters, σ_j and γ_j , are the pathogen shedding rate (infected-to-cloud) and decay rate in the cloud, respectively. Their estimates are provided in Appendix A.

Finally, the constant G formalizes the resource volume generated by working individuals per unit time. It is proportional to the average working time T_4 for the given social group (see Table II). The parameter Γ_ρ represents the resource consumption rate. The parameter Λ represents the fixed expenses necessary for keeping some infrastructure (e.g. amortization, municipal services, etc.).

Note that the instantaneous number density of quarantine (ill) individuals $q(t)$ is not often a convenient indicator for practical applications. The integrate number density of quarantine individuals for a certain period of time can be used instead. It is calculated as follows

$$q_\Sigma = \Gamma_{iq} \int_0^t i \, d\tau. \quad (18)$$

In the case of unlimited resource ($E = 0$), the integrate number density of quarantine individuals in the end of epidemic ($t \rightarrow \infty$) is proportional to the final number

density of fatal cases,

$$(q_\Sigma)_\infty = \eta f_\infty, \quad (19)$$

where η is the probability of the fatal scenario for the quarantine individual.

D. Analysis

For our further analysis, we first find the stationary solution to Eq. (16c) for the cloud j :

$$d_j^* = \frac{\sigma_j}{\gamma_j} i^*. \quad (20)$$

This relation allows us to introduce the dimensionless pathogen concentration in the cloud j , namely

$$p_j = \frac{\gamma_j}{\sigma_j} d_j, \quad (21)$$

so that $p_j^* = i^*$. Then Eqs. (16a) and (16c) can be rewritten as

$$\begin{aligned} \partial_t s &= -\left(\beta i + \sum_j \beta_j p_j\right) s + \Gamma_{is} i + \Gamma_{qs} e^{-E/\rho} q, \\ \partial_t i &= \left(\beta i + \sum_j \beta_j p_j\right) s - \Gamma_i i, \\ \partial_t q &= \Gamma_{iq} i - \Gamma_q q, \\ \partial_t r &= \Gamma_{ir} i + \Gamma_{qr} e^{-E/\rho} q, \\ \partial_t p_j &= \gamma_j (i - p_j), \end{aligned} \quad (22)$$

where β is the direct transmission rate (infected-to-susceptible) given by formula (14) and β_j are the scaled indirect transmission rates via each of the clouds j (infected-cloud-susceptible):

$$\beta_j = \nu_j \frac{T_j}{T}. \quad (23)$$

The scaled indirect transmission frequencies ν_j are defined as

$$\nu_j = \Omega_j \frac{\sigma_j}{\gamma_j}. \quad (24)$$

Equations (22) supplemented with Eqs. (16b) and (16d) possess two equilibrium points. The first one is the disease-free equilibrium

$$s^{(0)} = 1, \rho = \rho^{(0)}, i^{(0)} = q^{(0)} = r^{(0)} = f^{(0)} = p_j^{(0)} = 0, \quad (25)$$

with $\rho^{(0)}$ given by formula (3). The second one is the endemic equilibrium

$$s^* = \mathcal{R}_0^{-1}, \quad i^* = q^* = p_j^* = 0, \quad (26)$$

where the basic reproduction number \mathcal{R}_0 is defined as

$$\mathcal{R}_0 = \tau_i \sum_j (\omega_j + \nu_j) \frac{T_j}{T} = \frac{\beta + \beta_p}{\Gamma_i}, \quad (27)$$

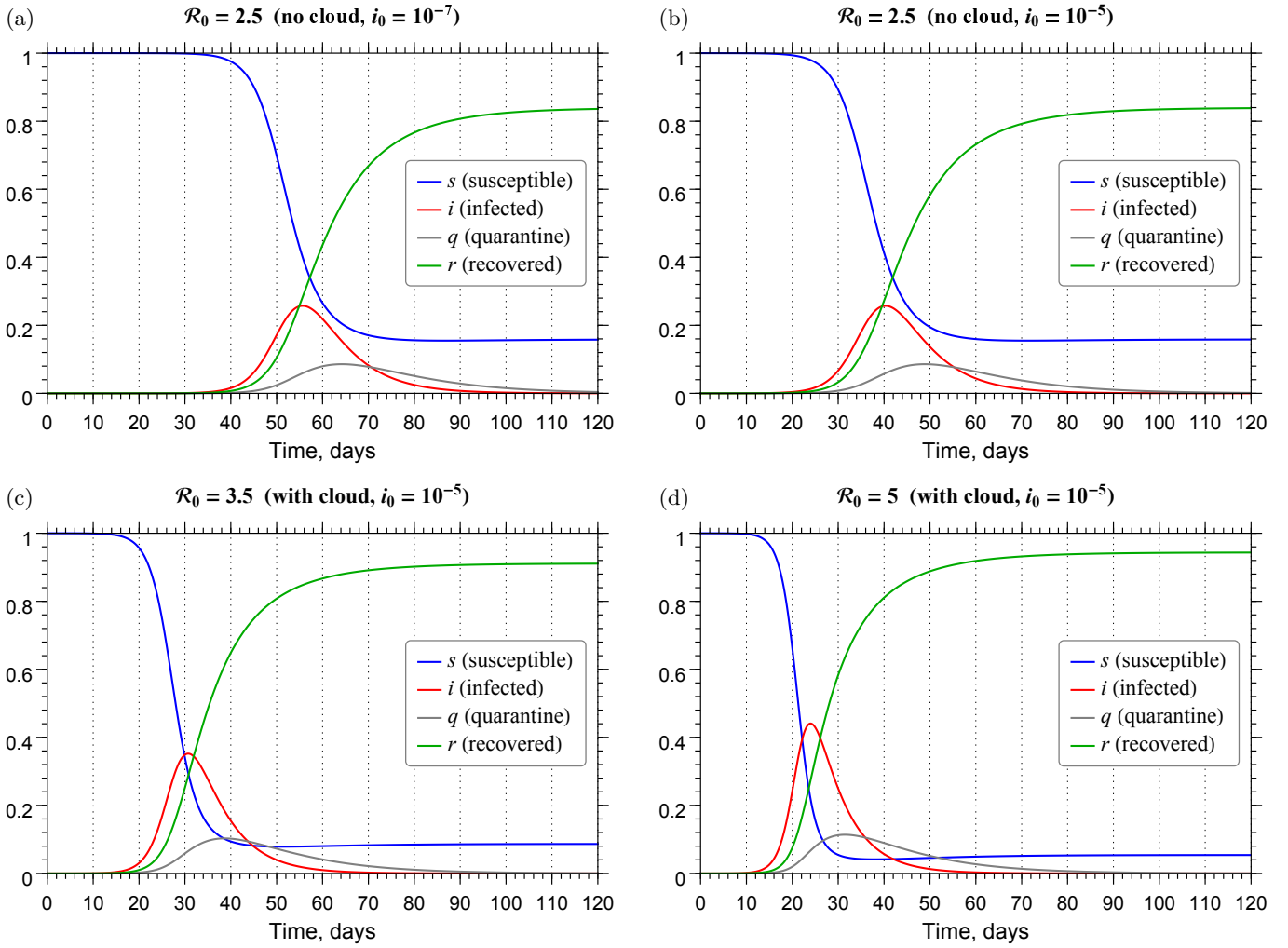


Figure 4. Effect of the cloud for the fixed $\beta = 0.5 T^{-1}$. (a) No cloud ($\beta_p = 0, i_0 = 10^{-7}$). (b) No cloud ($\beta_p = 0, i_0 = 10^{-5}$). (c) With cloud ($\beta_p = 0.2 T^{-1}, i_0 = 10^{-5}$). (d) With cloud ($\beta_p = 0.5 T^{-1}, i_0 = 10^{-5}$).

Table I. Main parameters of numerical solutions shown in Fig. 4.

β	β_p	\mathcal{R}_0	i_0	i_{\max}	$t_{i_{\max}}$, days	q_{\max}	$t_{q_{\max}}$, days	$(q_{\Sigma})_{\infty}$	s_{∞}
$0.5 T^{-1}$	0	2.5	10^{-7}	0.257	55.7	0.086	64.2	0.210	0.158
$0.5 T^{-1}$	0	2.5	10^{-5}	0.257	40.3	0.086	48.9	0.210	0.158
$0.5 T^{-1}$	$0.2 T^{-1}$	3.5	10^{-5}	0.352	30.7	0.103	38.6	0.228	0.087
$0.5 T^{-1}$	$0.5 T^{-1}$	5	10^{-5}	0.441	24.0	0.114	31.5	0.236	0.054
Quarantine scenario			10^{-5}	0.233	73.5	0.078	81.6	0.225	0.098

where

$$\beta_p = \sum_j \beta_j \quad (28)$$

is the aggregate indirect pathogen transmission rate via all the clouds. The parameter \mathcal{R}_0 represents the number of secondary cases generated if a single infected individual is introduced into a completely susceptible population.

When $\mathcal{R}_0 \leq 1$, the disease-free equilibrium is stable,

and there is no epidemic outbreak.

When $\mathcal{R}_0 > 1$, the disease-free equilibrium is unstable, and the system evolves to the state of endemic equilibrium.

The stationary points for the resource function, number density of recovered individuals, and the number den-

sity of fatal cases are given by the formulas

$$\rho^* = -E \log^{-1} \left(\frac{\Gamma_q (\Gamma_{iq} + \Gamma_{ir})}{\Gamma_{qs} \Gamma_{iq}} \right), \quad (29a)$$

$$r^* = \frac{\Gamma_\rho \rho^* - \Lambda}{G} - s^*, \quad (29b)$$

$$f^* = 1 - s^* - r^* = 1 - \frac{\Gamma_\rho \rho^* - \Lambda}{G}. \quad (29c)$$

The variable resource is seen to have a profound effect on the endemic number densities of the recovered individuals and fatal cases. However, in contrast to the example considered in Section II based on a simpler SIS-like model, our extended model is more stable in regard to the resource depletion and does not allow for the total collapse scenario with s and ρ vanishing to zero at $E \gg \rho$.

The first two equations of system (22) are strongly nonlinear. There are no analytical solutions known for the general form of these equations. However, in one particular case, when $\Gamma_{is} = \Gamma_{qs} = 0$ ($\mu = 1$, no loss of immunity) and $E = 0$ (unlimited resource), one can get the following asymptotics at $t \rightarrow \infty$:

$$\log \left(\frac{s(0)}{s_\infty} \right) = \mathcal{R}_0 (1 - s_\infty), \quad i_\infty = 0, \quad q_\infty = 0. \quad (30)$$

Equation (30) can be used to control the accuracy of the numerical integration of system (22). In the examples considered in the next Section, we used the fourth-order Runge-Kutta method to integrate Eqs. (22) numerically with step $\Delta t = T/10$ sufficient to achieve the reasonable accuracy. In the case $\mu = 1$ (no loss of immunity) our numerical estimate of s_∞ coincided with the value given by Eq. (30) to an accuracy of 10^{-10} .

V. EXAMPLES

Now we consider particular examples to demonstrate various effects described by our model. First we focus on the case when there is no resource depletion ($\rho \gg E$), so that the resource activation mechanism could be ignored ($E = 0$). We illustrate the “patient zero” phenomenon, then demonstrate the effect of the cloud, and finally model a quarantine scenario. Next we consider an example of a social group with limited resource ($E \neq 0$).

A. Effect of i_0

Figures 4(a,b) show the number densities of the susceptible, infected, quarantine, and recovered individuals as functions of time in the case of two different initial number densities of infected individuals i_0 for the fixed basic reproduction number ($\mathcal{R}_0 = 2.5$). Panel (a) corresponds to an initial density of one per 10 million, and panel (b) corresponds to an initial density of one per 100 thousand. The number density of infected individuals exhibits a typical peak and then drops. The peak has the

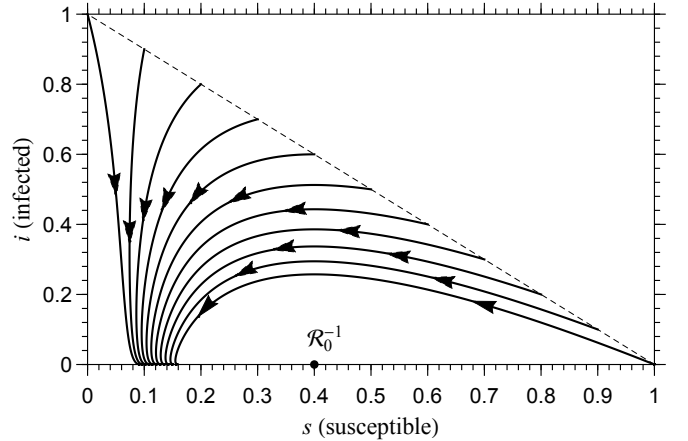


Figure 5. Susceptible-infected phase plane portrait for $\mathcal{R}_0 = 2.5$ and various initial number densities of infected individuals i_0 .

same height for the both initial densities, but in the case of larger i_0 it is reached much faster (see Table I). This example serves as an illustration of the “patient zero” phenomenon. When $\mathcal{R}_0 > 1$, the epidemic spreads even when it starts only from one infected individual (patient zero). Then it reaches the same intensity in a certain period of time, which is shorter when the initial number of infected individuals is larger. This effect is also clearly seen in the phase portraits $i(s)$ at different i_0 (Fig. 5).

B. Cloud effect

Figure 4 shows the number densities of susceptible, infected, quarantine, and recovered individuals in the cases when there is no indirect transmission [no cloud, panels (a) and (b)] and when there is such a transmission [with cloud, panels (c) and (d)]. The cloud parameters are listed in Table IV (Appendix A), and all other model parameters were selected according to Table III therein.

The corresponding parameters of the peaks are given in Table I. The inclusion of the cloud increased the basic reproduction number \mathcal{R}_0 , so that the peaks of infected (i_{\max}) and quarantine (q_{\max}) densities become larger and shift to shorter times. The total number density of quarantine individuals $(q_\Sigma)_\infty$ is significantly larger in the case with cloud.

C. Modelling the quarantine scenario

The epidemic dynamics is governed by the basic reproduction number \mathcal{R}_0 . The epidemic starts to spread when $\mathcal{R}_0 > 1$. The greater \mathcal{R}_0 , the higher are i_{\max} , q_{\max} , and $(q_\Sigma)_\infty$. Thus, to reduce the epidemic peak and to slow the epidemic down, one should reduce \mathcal{R}_0 . According to formula (27), this can be achieved by reducing the transmission frequencies ω_j and, therefore, the transmission

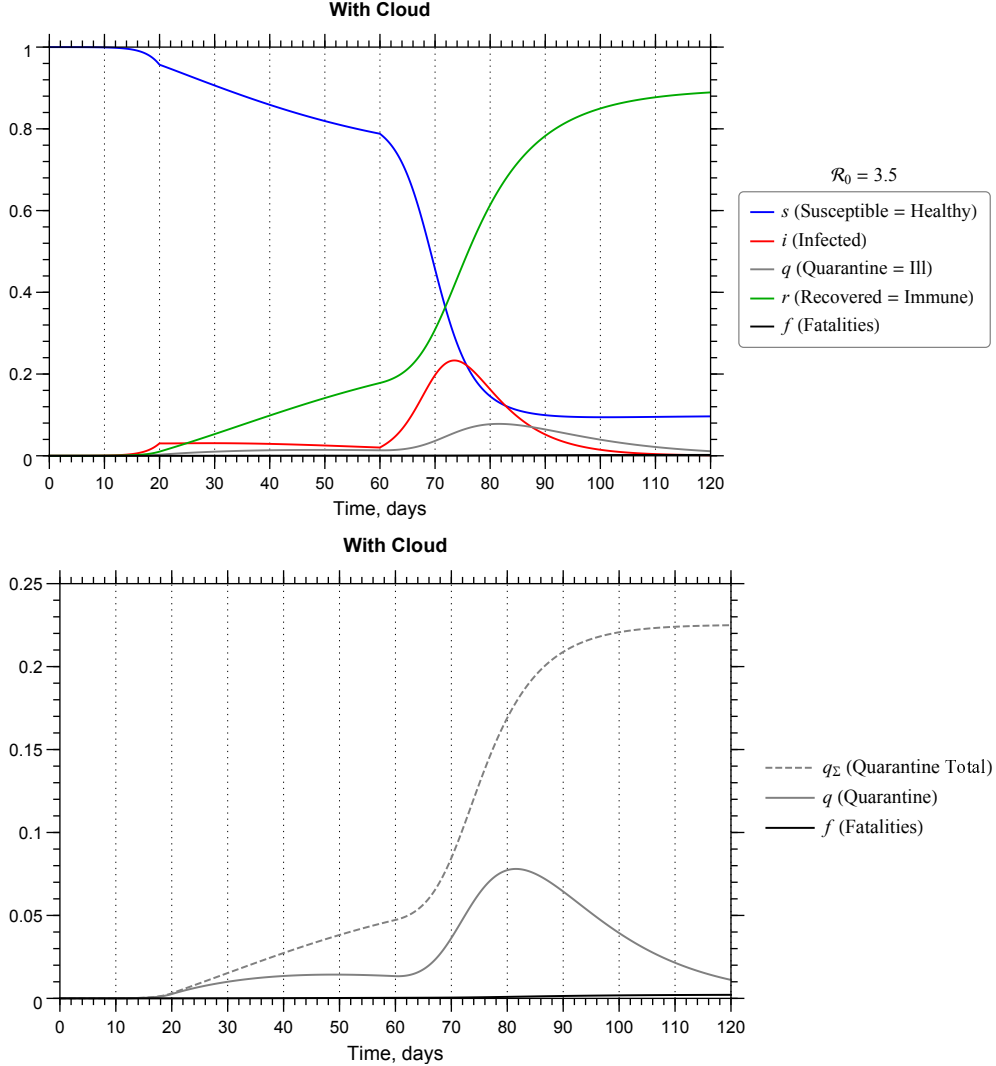


Figure 6. Modeling the quarantine scenario with $t_1 = 20T$, $t_2 = 60T$, $\beta^{(0)} = 0.5T^{-1}$, $\beta^{(1)} = 0.18T^{-1}$, $\beta_p^{(0)} = 0.2T^{-1}$, and $\beta_p^{(1)} = 0.04T^{-1}$.

Table II. Social control parameters and transmission rates at $\ell_0 = 1$ m, $\ell_c = 4$ m, and $\tau_{is} = T/3$.

Location	Description	T_j , h	$\bar{\ell}_j$, m	ω_j	T_j , h	$\bar{\ell}_j$, m	ω_j	T_j , h	$\bar{\ell}_j$, m	ω_j
$j = 1$	Home	11.5	3.5	$0.06T^{-1}$	12.5	3.5	$0.06T^{-1}$	19.5	3.5	$0.06T^{-1}$
$j = 2$	Shopping	1.5	1.5	$1.15T^{-1}$	1.5	2.25	$0.41T^{-1}$	0.5	2.25	$0.41T^{-1}$
$j = 3$	Transport	3	1	$2.81T^{-1}$	2	1.5	$1.15T^{-1}$	0		
$j = 4$	Work	8	3	$0.15T^{-1}$	8	3.25	$0.10T^{-1}$	4	3.25	$0.10T^{-1}$
β	Casual			$0.5T^{-1}$	Soft quarantine		$0.18T^{-1}$	Strict quarantine		$0.07T^{-1}$

rate β . Such measures are usually referred to as quarantine. To model the quarantine scenario, we assumed the

following form of the transmission coefficients:

$$\beta = \begin{cases} \beta^{(0)}, & t < t_1, \\ \beta^{(1)}, & t_1 \leq t < t_2, \\ \beta^{(0)}, & t \geq t_2, \end{cases} \quad \beta_p = \begin{cases} \beta_p^{(0)}, & t < t_1, \\ \beta_p^{(1)}, & t_1 \leq t < t_2, \\ \beta_p^{(0)}, & t \geq t_2, \end{cases} \quad (31)$$

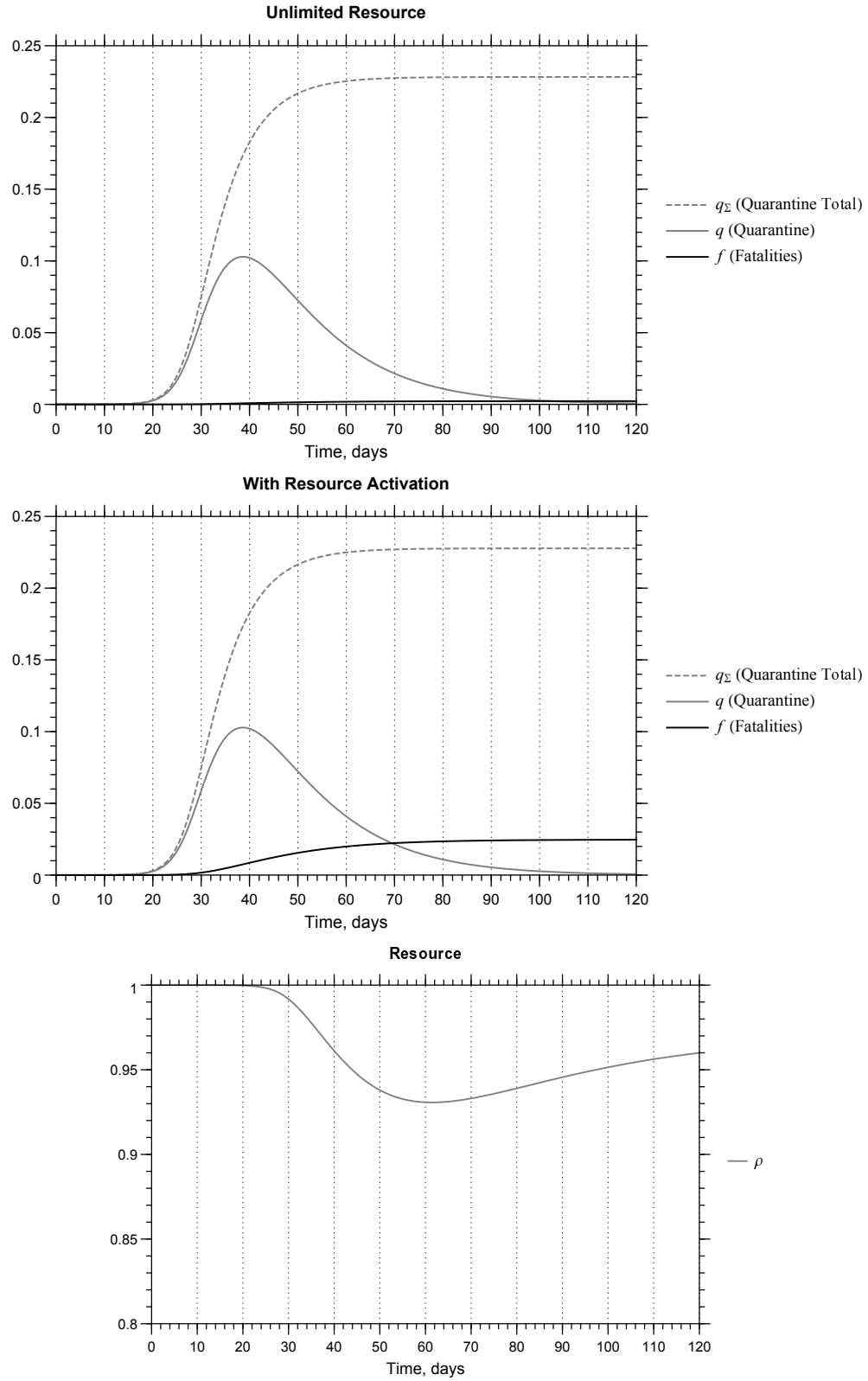


Figure 7. Effect of the resource function.

where t_1 is the moment when the quarantine starts, t_2 is the moment when the quarantine ends, $\beta^{(0)}$ and $\beta_p^{(0)}$ are the direct and indirect transmission rates during the “no quarantine” period, and $\beta^{(1)}$ and $\beta_p^{(1)}$ are the transmission rates during the quarantine period.

Figure 6 presents the results of our modeling. This example describes the scenario when the initial basic reproduction number $\mathcal{R}_0 = 3.5$ was reduced to $\mathcal{R}_0 = 1.1$ by the quarantine measures at $t_1 = 20$ days. The number density of quarantine individuals continued to grow but at much lesser rate and acquired a local peak at $t \approx 48$ days. Then the quarantine was terminated at $t_2 = 60$ days. The number densities of the infected and quarantine individuals immediately started to grow again and reached the new peaks that were much larger than those during the quarantine (row 5 in Table I). As compared to the “no quarantine” scenario (row 3 in Table I), the absolute heights of the peaks decreased, but the total number densities of quarantine individuals and fatal cases remained nearly the same. Thus, the quarantine scenario allows one to win time but does not seriously affect the total number of ill and deceased people, in the case when the fatality rate remains to be constant.

Our results are in line with the results of modeling presented in Ref. [22]. The greater the reduction in transmission, the longer and flatter is the epidemic curve, with the risk of resurgence when interventions are lifted to mitigate economic impact. The similar results were obtained when modeling the COVID-19 quarantine scenario for the Wuhan city, with a stochastic SEIR model fitted to the available statistical data [44]. The initial \mathcal{R}_0 value equal to 2.35 (the median estimate) before the quarantine restrictions took place declined to $\mathcal{R}_0 \approx 1.05$ after the start of the quarantine.

D. The resource activation mechanism

Finally, we demonstrate the effect of nonzero resource activation parameter E . Figure 7 demonstrates the effect of the resource function for $E = 0.1$, with all other parameters listed in Table III. The nonzero resource activation parameter E has a profound effect on the number of fatal cases. This example illustrates the scenario when the economic subsystem has no resource to support the medical infrastructure, so that seriously ill (quarantine) individuals could not get the necessary medical services to overcome the infection. However, in contrast to the toy example considered in Section II, dynamic system (22) does not collapse, the resource function exhibiting a clearly identified minimum with a subsequent surge.

VI. CONCLUSION

We proposed a novel approach for modeling the spread of epidemics. The spreading process within a selected social group is described by the dynamic equations which

explicitly account for the dependence of characteristic reaction (infection) rates on the local population density in various social zones. The indirect channel of infection transmission via an intermediate environment or the so-called fomites was also taken into account. Moreover, the model accounts for the negative feedback in the “epidemic–economic resource” system. To this end, the equations describing the spreading process were supplemented with equations for the formal economic resource. The epidemic spread and the use of quarantine measures was demonstrated to be connected with economic losses, which in turn can lead to the collapse of the system, at least for a number of industries and/or social groups.

Appendix A: Model parameters (extended)

Table II gives transmission frequencies ω_j and rates β calculated by formulas (12) and (14) for various sets of social control parameters.

Table III gives the full description of the model parameters and their estimates used in our computations.

In particular, the cloud-related parameters can be estimated as follows. The typical frequency Ω_j of the pathogen transmission from the cloud j to the susceptible individual can roughly be estimated as

$$\Omega_j = \Gamma_{js} \frac{v_c}{\Delta} \theta, \quad [\text{time}^{-1} \times \text{mass}^{-1} \times \text{volume}] \quad (\text{A1})$$

where Γ_{js} is the average rate the susceptible individual contacts the cloud j , v_c is a typical volume of the pathogen transferred from the cloud to the susceptible individual per one contact, Δ is some characteristic weight of one pathogen specimen that can be interpreted as the minimum portion (“quant”) of the pathogen that can be transferred per one contact), and θ is the probability the transmission of this quant results in infection. The smaller the pathogen, the smaller is the quant \hbar and the more intensive is transmission (Ω_j is higher). The parameters v_c , Δ , and θ are assumed to be independent of the particular cloud.

The pathogen shedding rate σ_j (infected-to-cloud) can roughly be estimated as

$$\sigma_j = \Gamma_{ij} \frac{n\Delta}{V_j}, \quad [\text{time}^{-1} \times \text{mass} \times \text{volume}^{-1}] \quad (\text{A2})$$

where Γ_{ij} is the average rate the infected individual contacts the cloud j (number of coughs, sneezes, touches, etc. per unit time), n is the typical number of the pathogen quants Δ transferred by the infected individual to the cloud per one contact, and V_j is the total volume (capacity) of the cloud j . The parameter n is assumed to be independent of the particular cloud.

Then the scaled indirect transmission frequencies ν_j can be estimated as

$$\nu_j = \Omega_j \frac{\sigma_j}{\gamma_j} = \frac{\Gamma_{ij} \Gamma_{js}}{\gamma_j} \chi_j. \quad (\text{A3})$$

Table III. Parameters of the model.

Description	Our model value	Literature data
β Direct transmission rate (infected-to-susceptible)	$0.5 T^{-1}$	$0.6 T^{-1}$ [37] [†] , $0.15 T^{-1}$ [38] [†]
ω_j Infected-to-susceptible transmission frequency for location j	see Table II	
β_j Indirect transmission rate (infected-cloud-susceptible) in cloud j	see Table IV	
β_p Aggregate indirect transmission rate (infected-cloud-susceptible)	$0.2 T^{-1}$	$0.35 T^{-1}$ [41] [‡]
ν_j Infected-cloud-susceptible transmission frequency in cloud j	see Eq. (A3)	
χ_j Infected-cloud-susceptible transmission efficiency in cloud j	10^{-5}	
γ_j Average pathogen decay rate in cloud j	τ_p^{-1}	
Γ_{js} Average contact rate (pickup) of susceptible individuals with cloud j	$240 T^{-1}$	$24\text{--}480 T^{-1}$ (fomites) [34]
Γ_{ij} Average contact rate (shedding) of infected individuals with cloud j	$360 T^{-1}$	$360 T^{-1}$ (coughs) [45] [§]
Γ_{iq} Infected-to-quarantine relaxation frequency	$(1 - \xi) \tau_i^{-1}$	
Γ_{ir} Infected-to-recovered relaxation frequency (with immunity)	$\xi \mu \tau_i^{-1}$	
Γ_{is} Infected-to-susceptible relaxation frequency (no immunity)	$\xi (1 - \mu) \tau_i^{-1}$	
Γ_i Total relaxation frequency for infected individuals, $\Gamma_{iq} + \Gamma_{ir} + \Gamma_{is}$	τ_i^{-1}	
Γ_{qr} Quarantine-to-recovered relaxation frequency (with immunity)	$\mu (1 - \eta) \tau_q^{-1}$	
Γ_{qs} Quarantine-to-susceptible relaxation frequency (no immunity)	$(1 - \mu) (1 - \eta) \tau_q^{-1}$	
Γ_{qf} Fatality rate in the case of unlimited resource	$\eta \tau_q^{-1}$	
Γ_q Total relaxation frequency for quarantine individuals, $\Gamma_{qr} + \Gamma_{qs} + \Gamma_{qf}$	τ_q^{-1}	
Γ_ρ Resource consumption rate	τ_ρ^{-1}	
T Unit of time	1 day	
T_j Average time spent in location j	see Table II	
ℓ_0 Minimum possible distance between two individuals	1 m	
ℓ_c Correlation radius (the maximum transmission distance)	4 m	
ℓ_j Average distance between individuals in location j	see Table II	
τ_{is} Characteristic time of becoming infected at close contact	$T/3$	
τ_p Average pathogen decay time outside the host	$2T$	$0.1\text{--}14 T^*$ [47] [†]
τ_i Average pathogen incubation period	$5T$	$3\text{--}10 T$ [46] [†] , $\approx 5 T$ [48, 49] [†]
τ_q Average quarantine/hospitalization time	$14T$	$(12.4 \pm 5) T$ [38] [†] , $14.5 T$ [50] [†]
τ_ρ Characteristic resource consumption time	$30T$	
ξ Probability for the infected individual to recover without quarantine	0.8	0.8^{**} [22] [†]
μ Probability of acquiring the immunity	0.8	
η Probability of the fatal scenario for the quarantine individual	0.01	0.014 [51, 52] [†]
E Normalized resource activation energy	0.1	
G Normalized resource volume per unit time	$(1 + \alpha) \Gamma_\rho$	
Λ Normalized infrastructure expenses per unit time	$\alpha \Gamma_\rho$	
α Infrastructure coefficient	0.2	
i_0 Initial number density of infected individuals	10^{-5}	

[†] for COVID-19[‡] for cholera outbreak[§] for pandemic influenza

* depends on medium, ambient temperature, and surface type

** 80% of COVID-19 cases are mild or asymptomatic

The dimensionless parameter

$$\chi_j = \frac{v_c}{V_j} n \theta \quad (\text{A4})$$

defines the transmission efficiency from the infected individual to the susceptible individual through the cloud j . Although the abstract parameter Δ was eliminated by scaling (21), the expression for χ_j still contains the

parameters that are hard to estimate from some physical principles. Therefore, this parameter can rather be estimated by fitting the model to some real statistical data. In practice, it is selected by assuming that the indirect and direct routes transmissions have approximately the same likelihood, i.e. $\nu_j \approx \omega_j$ [32].

Table IV gives indirect transmission frequencies ν_j and rates β_j calculated by formulas (A3) and (23) for a par-

Table IV. Indirect transmission frequencies and rates.

Cloud	T_j , h	$\bar{\ell}_j$, m	Γ_{js}	ν_j	β_j
$j = 1$	11.5	3.5	$20 T^{-1}$	$0.14 T^{-1}$	$0.02 T^{-1}$
$j = 2$	1.5	1.5	$107 T^{-1}$	$0.77 T^{-1}$	$0.10 T^{-1}$
$j = 3$	3	1	$240 T^{-1}$	$1.73 T^{-1}$	$0.22 T^{-1}$
$j = 4$	8	3	$27 T^{-1}$	$0.19 T^{-1}$	$0.02 T^{-1}$

Table V. Available estimates of \mathcal{R}_0 for COVID-19.

\mathcal{R}_0	Reference	Data source
1.5–3.5	Imai et al. [53]	Wuhan
2.4–4.1	Read et al. [54]	Wuhan
2.2–3.6	Zhao et al. [55]	Wuhan
1.4–3.9	Li et al. [49]	Wuhan
2.5–2.9	Wu et al. [56]	Wuhan

ticular set of social control parameters. The contact infected-to-cloud rates Γ_{ij} , pathogen decay rates γ_j , and transmission efficiencies χ_j are assumed to be the same for each cloud and listed in Table III. The contact cloud-to-susceptible rate Γ_{js} is assumed to be inversely proportional to the squared social distance ℓ_j between the individuals [as in Eq. (12)].

Table V lists some estimates of the basic reproduction number \mathcal{R}_0 derived from the statistical data on COVID-19 (literature data).

[1] R. Pastor-Satorras, C. Castellano, P.V. Mieghem, and A. Vespignani, Epidemic processes in complex networks, *Rev. Mod. Phys.* **87**, 925–979 (2015).

[2] S. Moore and T. Rogers, Predicting the speed of epidemics spreading in networks, *Phys. Rev. Lett.* **124**, 068301 (2020).

[3] N. Masuda and P. Holme, Small inter-event times govern epidemic spreading on networks, *Phys. Rev. Res.* **2**, 023163 (2020).

[4] J.A.T. Machado and A.M. Lopes, Rare and extreme events: the case of COVID-19 pandemic, *Nonlinear Dynamics* **100**, 2953–2972 (2020).

[5] P. Cirillo and N.N. Taleb, Tail risk of contagious diseases, *Nat. Phys.*, published online (2020). <https://doi.org/10.1038/s41567-020-0921-x>

[6] N.T.J. Bailey, Macro-modelling and prediction of epidemic spread at community level. *Mathematical Modelling* **7**, 689–717 (1986).

[7] H.W. Hethcote, The mathematics of infectious diseases. *SIAM Review* **42**(4), 599–653 (2000).

[8] D. Bichara, Y. Kang, C. Castillo-Chavez, R. Horan, and C. Perrings, SIS and SIR epidemic models under virtual dispersal. *Bull. Math. Biol.* **77**, 2004–2034 (2015).

[9] N. Bacaër, *A Short History of Mathematical Population Dynamics* (Springer, London, 2011).

[10] M. Martcheva, *An Introduction to Mathematical Epidemiology* (Springer, New York, 2015).

[11] F. Brauer, C. Castillo-Chavez, and Z. Feng, *Mathematical Models in Epidemiology* (Springer, New York, 2019).

[12] T. Hasegawa and K. Nemoto, Outbreaks in susceptible-infected-removed epidemics with multiple seeds, *Phys. Rev. E* **93**, 032324 (2016).

[13] S. Maslov and K. Sneppen, Severe population collapses and species extinctions in multihost epidemic dynamics, *Phys. Rev. E* **96**, 022412 (2017).

[14] D. Bernoulli, Essai d'une nouvelle analyse de la mortalité causée par la petite vérole, *Mem. Math. Phys. Acad. R. Sci. Paris*, 1–45 (1766) [English translation entitled “An attempt at a new analysis of the mortality caused by smallpox and of the advantages of inoculation to prevent it” in: L. Bradley, *Smallpox Inoculation: An Eighteenth Century Mathematical Controversy* (Adult Education Department, Nottingham, 1971), p. 21. Reprinted in: S. Haberman and T.A. Sibbett (Eds.), *History of Actuarial Science. Vol. VIII: Multiple Decrement and Multiple State Models* (William Pickering, London, 1995), p. 1.; S. Blower, *Rev. Med. Virol.* **14**, 275–288 (2004)]; J. de l'Écambert, Sur l'application du calcul des probabilités à l'inoculation de la petite vérole. In: *Opuscules mathématiques*, t. 2 (David, Paris, 1761), p. 26–95; K. Dietz and J.A.P. Heesterbeek, Daniel Bernoulli's epidemiological model revisited. *Mathematical Biosciences* **180**, 1–21 (2002).

[15] R. Ross, *The Prevention of Malaria*, 2nd edn. (John Murray, London, 1911).

[16] W.O. Kermack and A.G. McKendrick, A contribution to the mathematical theory of epidemics. *Proc. Roy. Soc. Lond. A* **115**, 700–721 (1927).

[17] W.O. Kermack and A.G. McKendrick, Contributions to the mathematical theory of epidemics. II.—The problem of endemicity. *Proc. Roy. Soc. Lond. A* **138**, 55–83 (1932).

[18] W.O. Kermack and A.G. McKendrick, Contributions to the mathematical theory of epidemics. III.—Further studies of the problem of endemicity. *Proc. Roy. Soc. Lond. A* **141**, 94–112 (1933).

[19] R.R. Wilkinson and K.J. Sharkey, Impact of the infectious period on epidemics, *Phys. Rev. E* **97**, 052403 (2018).

[20] V. Colizza, R. Pastor-Satorras, and A. Vespignani, Reaction-diffusion processes and metapopulation models in heterogeneous networks, *Nat. Phys.* **3**, 276–282 (2007).

[21] S. Yu, Z. Yu, H. Jiang, X. Mei, and J. Li, The spread and control of rumors in a multilingual environment, *Nonlinear Dynamics* **100**, 2933–2951 (2020).

[22] R.M. Anderson, H. Heesterbeek, D. Klinkenberg, and T.D. Hollingsworth, How will country-based mitigation measures influence the course of the COVID-19 epi-

demic? *Lancet* **395**, 931–934 (2020).

[23] C.T. Bauch and D.J.D. Earn, Vaccination and the theory of games, *PNAS* **101**(36), 13391–13394 (2004).

[24] H. Hu, K. Nigmatulina, and P. Eckhoff, The scaling of contact rates with population density for the infectious disease models. *Mathematical biosciences* **244**, 125–134 (2013).

[25] C. Perrings, C. Castillo-Chavez, G. Chowell, P. Daszak, E.P. Fenichel, D. Finnoff, R.D. Horan, A.M. Kilpatrick, A.P. Kinzig, N.V. Kuminoff, S. Levin, B. Morin, K.F. Smith, and M. Springborn, Merging economics and epidemiology to improve the prediction and management of infectious disease, *EcoHealth* **11** 464–475 (2014).

[26] K.J. Laidler, *Chemical Kinetics*, 3rd ed. (Harper & Row., 1987).

[27] W. Stiller, *Arrhenius Equation and Non-Equilibrium Kinetics: 100 Years Arrhenius Equation* (BG Teubner Verlagsgesellschaft, 1989).

[28] S. Glasstone, K.J. Laidler, and H. Eyring, *The Theory of Rate Processes: The Kinetics of Chemical Reactions, Viscosity, Diffusion and Electrochemical Phenomena* (McGraw-Hill, 1941).

[29] B.M. Smirnov, Energetic processes in macroscopic fractal structures, *Sov. Phys. Usp.* **34**, 526–541 (1991).

[30] D.A. Frank-Kamenetskii, *Diffusion and Heat Transfer in Chemical Kinetics* (Plenum Press, N.Y., 1969).

[31] Ya.B. Zel'dovich and D.A. Frank-Kamenetskii, On the theory of uniform flame propagation, *Dokl. Adad. Nauk SSSR* **19**, 693–698 (1938) [in Russian].

[32] J.H. Tien and D.J.D. Earn, Multiple transmission pathways and disease dynamics in a waterborne pathogen model. *Bulletin of Mathematical Biology* **72**, 1506–1533 (2010).

[33] Z. Shuai and P. van den Driessche, Global dynamics of cholera models with differential infectivity. *Mathematical Biosciences* **234**, 118–126 (2011).

[34] S. Li, J.N.S. Eisenberg, I.H. Spicknall, and J.S. Koopman, Dynamics and control of infections transmitted from person to person through the environment. *Am. J. Epidemiol.* **170**(2), 257–265 (2009).

[35] A.N.M. Kraay, M.A.L. Hayashi, N. Hernandez-Ceron, I.H. Spicknall, M.C. Eisenberg, R. Meza, and J.N.S. Eisenberg, Fomite-mediated transmission as a sufficient pathway: a comparative analysis across three viral pathogens. *BMC Infectious Diseases* **18**, 540 (2018).

[36] P. Bak, The Devil's staircase. *Physics Today* **39**(12), 38–45 (1986).

[37] W.C. Roda, M.B. Varughese, D. Han, and M.Y. Li, Why is it difficult to accurately predict the COVID-19 epidemic? *Infectious Disease Modelling* **5**, 271–281 (2020).

[38] H. Wang, Z. Wang, Y. Dong, R. Chang, C. Xu, X. Yu, S. Zhang, L. Tsamlag, M. Shang, J. Huang, Y. Wang, G. Xu, T. Shen, X. Zhang, Y. Cai, Phase-adjusted estimation of the number of coronavirus disease 2019 cases in Wuhan, China. *Cell Discovery* **6**, 10 (2020).

[39] A.C. Osemwinyen and A. Diakhaby, Mathematical modelling of the transmission dynamics of Ebola virus. *Applied and Computational Mathematics* **4**, 313–320 (2015).

[40] Z. Feng and H.R. Thieme, Recurrent outbreaks of childhood diseases revisited: the impact of isolation. *Mathematical Biosciences* **128**, 93–130 (1995).

[41] M.C. Eisenberg, S.L. Robertson, and J.H. Tien, Identifiability and estimation of multiple transmission pathways in cholera and waterborne disease. *Journal of Theoretical Biology* **324**, 84–102 (2013).

[42] F. Brauer, A new epidemic model with indirect transmission. *Journal of Biological Dynamics* **11**, 285–293 (2017).

[43] J.F. David, Epidemic models with heterogeneous mixing and indirect transmission. *Journal of Biological Dynamics* **12**, 375–399 (2018).

[44] A.J. Kucharski, T.W. Russell, C. Diamond, Y. Liu, J. Edmunds, S. Funk, R.M. Eggo, Early dynamics of transmission and control of COVID-19: a mathematical modelling study. *Lancet Infect. Dis.* **20**, 553–558 (2020).

[45] M.P. Atkinson and L.M. Wein, Quantifying the routes of transmission for pandemic influenzas. *Bulletin of Mathematical Biology* **70**, 820–867 (2008).

[46] J. Chen, Pathogenicity and transmissibility of 2019-nCoV—A quick overview and comparison with other emerging viruses. *Microbes and Infection* **22**, 69–71 (2020).

[47] A.W.H. Chin, J.T.S. Chu, M.R.A. Perera, K.P.Y. Hui, H.-L. Yen, M.C.W. Chan, M. Peiris, and L.L.M. Poon, Stability of SARS-CoV-2 in different environmental conditions. *Lancet Microbe* **1**, e10 (2020).

[48] S.A. Lauer, K.H. Grantz, Q. Bi, F.K. Jones, Q. Zheng, H.R. Meredith, A.S. Azman, N.G. Reich, J. Lessler, The incubation period of coronavirus disease 2019 (COVID-19) from publicly reported confirmed cases: estimation and application. *Ann. Intern. Med.* **172**(9), 577–583 (2020).

[49] Q. Li et al., Early transmission dynamics in Wuhan, China, of novel coronavirus-infected pneumonia. *N. Engl. J. Med.* **382**(13), 1199–1207 (2020).

[50] K. Gaythorpe et al., Symptom progression of COVID-19. Report 8 of the Imperial College London COVID-19 Response Team (2020), <https://doi.org/10.25561/77344>.

[51] J.T. Wu, K. Leung, M. Bushman, N. Kishore, R. Niehus, P.M. de Salazar, B.J. Cowling, M. Lipsitch, and G.M. Leung, Estimating clinical severity of COVID-19 from the transmission dynamics in Wuhan, China. *Nature Medicine* **26**, 506–510 (2020).

[52] R. Verity, Estimates of the severity of coronavirus disease 2019: a model-based analysis. *Lancet Infect. Dis.*, Published online (2020), [https://doi.org/10.1016/S1473-3099\(20\)30243-7](https://doi.org/10.1016/S1473-3099(20)30243-7).

[53] N. Imai, A. Cori, I. Dorigatti, M. Baguelin, C.A. Donnelly, S. Riley, N.M. Ferguson, Transmissibility of 2019-nCoV. Report 3 of the Imperial College London COVID-19 Response Team (2020), <https://doi.org/10.25561/77148>.

[54] J.M. Read, J.R.E. Bridgen, D.A.T. Cummings, A. Ho, C.P. Jewell, Novel coronavirus 2019-nCoV: early estimation of epidemiological parameters and epidemic predictions. *MedRxiv* preprint (2020), <https://doi.org/10.1101/2020.01.23.20018549>.

[55] S. Zhao, Q. Linc, J. Rand, S.S. Musae, G. Yang, W. Wangh, Y. Loue, D. Gaoi, L. Yangj, D. Hee, and M.H. Wanga, Preliminary estimation of the basic reproduction number of novel coronavirus (2019-nCoV) in China, from 2019 to 2020: A data-driven analysis in the early phase of the outbreak. *International Journal of Infectious Diseases* **92**, 214–217 (2020).

[56] J.T. Wu, K. Leung, G.M. Leung, Nowcasting and forecasting the potential domestic and international spread of the 2019-nCoV outbreak originating in Wuhan, China: a modelling study. *Lancet* **395**, 689–697 (2020).

[57] Will be published elsewhere soon.